THE JOURNAL OF BIOLOGICAL CHEMISTRY VOL. 288, NO. 47, pp. 33509–33518, November 22, 2013

17β-Estradiol Inhibits Phosphorylation of Stromal Interaction Molecule 1 (STIM1) Protein

*IMPLICATION FOR STORE-OPERATED CALCIUM ENTRY AND CHRONIC LUNG DISEASES**

Received for publication, May 17, 2013, and in revised form, October 9, 2013 Published, JBC Papers in Press, October 10, 2013, DOI 10.1074/jbc.M113.486662

John T. Sheridan[‡1], Rodney C. Gilmore[§], Michael J. Watson[§], Christopher B. Archer[§], and Robert Tarran[‡§2]

From the [‡]Department of Cell and Molecular Physiology and the [§]Cystic Fibrosis/Pulmonary Research and Treatment Center, the University of North Carolina, Chapel Hill, North Carolina 27599

Background: It is unclear how acute exposure to estrogen inhibits Ca^{2+} influx and Ca^{2+}-activated Cl^- secretion in airway epithelia.
Results: Estrogen inhibited oligomerization and basal phosphorylation of STIM1, a key regulator of Ca^{2+} influx.
Conclusion: Acute exposure to estrogen inhibits Ca^{2+} influx by disrupting STIM1.
Significance: Knowing how estrogen inhibits Ca^{2+} signaling in the airways increases our understanding of sex-specific differences in lung diseases.

Sex plays a significant role in the development of lung diseases including asthma, cancer, chronic bronchitis, and cystic fibrosis. In cystic fibrosis, 17β-estradiol (E2) may inhibit store-operated Ca^{2+} entry (SOCE) to impinge upon airway secretions, leaving females at greater risk of contracting lung infections. Stromal interaction molecule 1 (STIM1)-mediated SOCE is essential for cell homeostasis and regulates numerous processes including cell proliferation, smooth muscle contraction, and secretion. E2 can signal nongenomically to modulate Ca^{2+} signaling, but little is known of the underlying mechanisms. We found that E2 exposure inhibited STIM1 translocation in airway epithelia, preventing SOCE. This correlated with a decrease in STIM1-STIM1 FRET and STIM1 mobility in E2-exposed HEK293T cells co-expressing estrogen receptor α. We also examined the role of STIM1 phosphorylation in E2-mediated inhibition of STIM1 mobility. STIM1 is basally phosphorylated at serine 575, which is required for SOCE. Exposure to E2 significantly decreased STIM1 serine phosphorylation. Mutating serine 575 to an alanine blocked STIM1 phosphorylation, reduced basal STIM1 mobility, and rendered STIM1 insensitive to E2. These data indicate that E2 can signal nongenomically by inhibiting basal phosphorylation of STIM1, leading to a reduction in SOCE.

Calcium is an important second messenger that controls cellular processes as varied as contraction, ion transport, regulation of transcription, growth, and cell division (1). Thus, precise regulation of cytoplasmic Ca^{2+} is required to maintain normal cellular homeostasis. This is achieved mainly by sequestering Ca^{2+} to internal stores, such as the endoplasmic reticulum (ER)[3] and mitochondria (2). Following receptor-mediated ER Ca^{2+} depletion, store-operated Ca^{2+} entry (SOCE) is used to further modulate cytoplasmic Ca^{2+} levels and to replenish depleted stores (3). SOCE requires the ER Ca^{2+}-sensing protein stromal interaction molecule 1 (STIM1) (4, 5) and the Ca^{2+} release-activated Ca^{2+} channel subunit Orai1 (6, 7). The N-terminal domain of STIM1 contains an EF-hand that protrudes into the lumen of the ER and senses changes in ER Ca^{2+} levels (3, 8). Upon depletion of ER Ca^{2+}, STIM1 undergoes a conformational change and oligomerizes into puncta at the ER-plasma membrane junction, where it activates Orai1 to induce Ca^{2+} influx (3, 8). In airway epithelia, one important consequence of agonist-dependent increases in $[Ca^{2+}]_i$ is the subsequent activation of transepithelial Cl^- secretion through the Ca^{2+}-activated Cl^- channel (CaCC). In patients with cystic fibrosis (CF), who the lack the CF transmembrane conductance regulator (CFTR) Cl^- channel, CaCC is still present and represents a "rescue" channel that may help maintain airway hydration in the absence of the CFTR (9).

Gender can greatly influence lung health (10). For example, CF women have a poorer prognosis and are more likely to experience an acute exacerbation than CF men (11, 12). Additionally, adult women are more likely to be diagnosed with early onset chronic obstructive pulmonary disease (COPD) (13), asthma (14), and adenocarcinoma of the lung (15). We have previously shown that 17β-estradiol (E2) inhibits agonist-mediated Ca^{2+} signaling through estrogen receptor α (ESR1) in a nongenomic fashion in airway epithelia, which ultimately prevents CaCC activation and leads to airway dehydration (16). Here, we tested the hypothesis that E2 inhibits key components of SOCE. We found that STIM1 was specifically inhibited by

* This work was supported by the Cystic Fibrosis Foundation, British American Tobacco, and National Institutes of Health Grants RO1 HL-10927 and PPG HL-034322.
[1] Supported by the Dr. Susan Fellner physiology graduate student research fellowship and the Howard Hughes Medical Institute Med-into-Grad University of North Carolina program in translational medicine.
[2] To whom correspondence should be addressed. Tel.: 919-966-7052; Fax: 919-966-5178; E-mail: tarran@med.unc.edu.

[3] The abbreviations used are: ER, endoplasmic reticulum; ANOVA, analysis of variance; Bis-Tris, Bis (2-hydroxyethyl) imino-tirs (hydroxymethyl) methane-HCl; CaCC, Ca^{2+}-activated Cl^- channel; CF, cystic fibrosis; CFP, cyan fluorescent protein; COPD, chronic obstructive pulmonary disease; E2, 17β-estradiol; ESR1, estrogen receptor α; FRAP, fluorescent recovery after photobleaching; HBEC, human bronchial epithelial cell; SOCE, store-operated Ca^{2+} entry; STIM1, stromal interaction molecule 1; TG, thapsigargin; TRP, transient receptor potential.

E2/ESR1, leading to an inhibition of SOCE but not ER Ca^{2+} release.

EXPERIMENTAL PROCEDURES

Chemicals and Reagents—17β-Estradiol and all salts and buffers were obtained from Sigma-Aldrich. Thapsigargin, Fura-2/AM, and phalloidin were obtained from Life Technologies. Antibodies were from Abcam (anti-GFP, also recognizes YFP), Millipore (anti-mpm-2), and Sigma-Aldrich (anti-STIM1). cDNAs encoding YFP-tagged STIM1 and 570STOP-STIM1 (truncation mutant) were kindly provided by T. Meyers (Stanford, CA) and J. Putney (NIEHS, NC), respectively. mCherry-tagged STIM1 was created by replacing the YFP tag on STIM1 with mCherry. ESR1-CFP was kindly provided by R. Day (University of Virginia) and subsequently tagged with mOrange. Orai1-YFP and EB1-GFP constructs were purchased from Addgene (19756 and 39299, respectively).

Cell Culture and Transfections—Human excess donor lungs and excised recipient lungs were obtained at the time of lung transplantation from portions of main stem or lumbar bronchi, and cells were harvested by enzymatic digestion as described previously under a protocol approved by the University of North Carolina Institutional Review Board (17). Human bronchial epithelial cells (HBECs) were plated on either glass coverslips to perform siRNA knockdown experiments or on polyester membrane Transwells (Corning) to induce polarization. HBECs that were plated on Transwells were grown in an air-liquid interface for 3 weeks prior to experiments. HEK293T cells were maintained in minimum Eagle's medium α supplemented with 10% fetal bovine serum and 1× penicillin/streptomycin solution. HEK293T cells were typically used 2–3 days after seeding. Cultures were transfected for 4–6 h using Lipofectamine 2000 (Life Technologies) according to the manufacturer's instructions. After transfecting, cultures were washed and placed in phenol-free medium and allowed to incubate in 5% CO_2 at 37 °C overnight.

siRNA Knockdown—STIM1 and Orai1 were transiently knocked down in HBECs using the Amaxa Nucleofector system according to the manufacturer's instructions with at least two different siRNA sequences obtained from Dharmacon. STIM1 and Orai1 knockdown were verified by quantitative PCR and at the functional level by measuring changes in intracellular Ca^{2+} with Fura-2.

Measurements of Intracellular Ca^{2+}—Intracellular Ca^{2+} imaging experiments were performed as described previously (16). Briefly, HEK293T and nonpolarized HBEC cultures were loaded with 2 μM Fura-2 AM at 37 °C for 15 min. Polarized HBECs were loaded with 5 μM Fura-2 AM while in the presence of 1 mM probenecid at 37 °C for 1 h. Cultures were washed with a standard Ringer's solution and then with Ca^{2+}-free Ringer's solution. Cultures were then placed in Ca^{2+}-free Ringer's solution, and images were collected with a 60 × 1.2 NA water objective on a Nikon Ti-S inverted microscope. Fura-2 fluorescence was acquired alternately at 340 and 380 nm (emission >450 nm) using LUDL filter wheels, obtained with an Orca CCD camera (Hammamatsu), and controlled with SimplePCI software. Background light levels were measured and subtracted from the corresponding signal measured in Fura-2-loaded cells before calculating the ratio (340/380). The background light levels in polarized HBECs were obtained by measuring the signals in non-Fura-2-loaded HBECs.

Immunofluorescence—Polarized HBECs were fixed bilaterally with 4% paraformaldehyde for 30 min at room temperature. After washing three times with PBS, HBECs were permeabilized with 0.1% Triton X-100 for 10 min and incubated in blocking buffer (1% IgG-free BSA, 1% normal goat serum) at room temperature for 1 h. HBECs were then incubated with an antibody against STIM1 in blocking buffer overnight at 4 °C. After washing with PBS, HBECs were incubated with Alexa Fluor 568 goat anti-rabbit secondary antibody (Life Technologies) for 1 h at room temperature. Actin was stained with phalloidin-488 (Invitrogen) according to the manufacturer's instructions. All antibodies and stains were applied bilaterally. Images were analyzed using ImageJ (National Institutes of Health).

STIM1 Puncta Quantification—HEK293T cells expressing STIM1-mCherry and ESR1-CFP were treated with vehicle, thapsigargin (TG), E2, or E2 + TG and then fixed with 4% paraformaldehyde for 10 min at room temperature. Each culture was assigned a random number that was unknown to the researcher to reduce bias. Multiple images were collected, and each cell was visually analyzed. A cell was deemed positive for puncta if any puncta were visible.

Confocal Microscopy Assays—A Leica SP5 confocal microscope with a 63× glycerol immersion objective was used for all confocal-based assays. Acceptor-photobleaching fluorescence resonance energy transfer (FRET) studies were performed on HEK293T cells expressing ESR1-CFP, STIM1-YFP, and STIM1-mCherry as described previously (18). Basal FRET was measured in cells that were treated with dimethyl sulfoxide vehicle or 10 nM E2 for 15 min. 2 μM thapsigargin was used to deplete ER-Ca^{2+} stores, and FRET measurements were collected. FRET images were analyzed using ImageJ. The FRET efficiency (%E) was calculated as: $((\text{dono}^{\text{postbleach}} - \text{donor}^{\text{prebleach}})/\text{donor}^{\text{postbleach}})*100$. Fluorescent recovery after photobleaching (FRAP) was measured in HEK293T cells expressing ESR1-mOr and YFP-STIM1, YFP-$STIM1^{570STOP}$, or YFP-$STIM1^{S575A}$, unless stated otherwise. Prebleach images were obtained before a circular region of interest was bleached. Subsequent images were collected every 30 s until maximum recovery had occurred. STIM1 FRAP curves were calculated by measuring the average fluorescence intensity in the bleached region of interest per time point and dividing it by the average fluorescence intensity of a nonbleached region of interest within the same cell per time point. To account for variations in protein expression and photobleaching, the average intensity ratio was normalized to the initial prebleach ratio.

Immunoprecipitation and Western Blotting—Immunoprecipitation was performed in HEK293T cells transfected with ESR1-mOrange and YFP-STIM1 or YFP-STIM1–570STOP truncation mutant ($STIM1^{570STOP}$). Cells were washed in 500 μl of Nonidet P-40 lysis buffer (0.1% Nonidet P-40, 50 mM Tris-HCl, pH 7.4, 10 mM $NaMoO_4$, 150 mM NaCl) supplemented with 1× complete EDTA-free protease inhibitors (Roche Applied Science) and 2× Halt phosphatase inhibitor mixture (Thermo Scientific). Lysates were then centrifuged at 16,000 × *g* for 10 min at 4 °C, and the supernatants were collected. Pro-

tein concentrations were determined by the BCA protein assay kit (Pierce), and equal amounts of protein (600 μg) were diluted to 1.2 μg μl^{-1} with Nonidet P-40 lysis buffer in spin columns (Pierce) and mixed with anti-GFP polyclonal antibody (Abcam; 1:500) and rotated at 4 °C overnight. Protein A/G-agarose beads (30 μl; Pierce) were added to lysate and rotated at 4 °C for 4 h. Beads were washed three times with Nonidet P-40 lysis buffer and centrifuged at 1000 × *g* for 2 min at 4 °C, and protein was eluted by boiling in sample buffer (2× NuPAGE LDS sample buffer and 1× reducing agent (Life Technologies)). Protein was resolved on a 4–12% gradient NuPAGE Bis-Tris gels (Life Technologies) and transferred to nitrocellulose using iBlot (Life Technologies). For Western blotting, immunoblots were blocked in 3% BSA in PBS-T for 1 h at room temperature, incubated overnight at 4 °C with primary antibodies (anti-mpm-2, 1:500 (Millipore); anti-GFP 1:2000 (Abcam), and incubated with secondary antibodies (horseradish peroxidase-linked anti-mouse or ant-rabbit 1:10,000 (GE Healthcare)) for 1 h at room temperature. Proteins were detected using SuperSignal West Pico or Femto Chemiluminescent Substrate kit (Pierce).

Statistical Analysis—All experiments were conducted on at least three separate occasions. Data were analyzed using the method stated in the figure legend. All statistical analyses were calculated using GraphPad Prism software.

RESULTS

E2 Inhibits Apical Ca^{2+} Influx in Human Bronchial Epithelial Cells—We have shown previously that E2 indirectly inhibits ligand-evoked Ca^{2+}-activated Cl^- secretion due to a reduction in Ca^{2+} signaling in human airway epithelia (16). To test whether this depression of cytoplasmic Ca^{2+} was due to an E2-mediated reduction in SOCE, we performed Ca^{2+} imaging experiments in polarized, Fura-2-loaded HBECs. HBECs were placed in Ca^{2+}-free Ringer's bilaterally and treated apically with thapsigargin (2 μM) to deplete ER Ca^{2+} (Fig. 1*A*). Because E2 would physiologically reach the epithelium through the blood, we applied it basolaterally. A 15-min pretreatment with E2 (10 nM) had no effect on ER Ca^{2+} release (Fig. 1*A*). We then added 2 mM Ca^{2+} to the apical surface to induce SOCE. Cells that were pretreated with E2 displayed a significantly reduced change in the Fura-2 ratio emission upon Ca^{2+} addition relative to untreated cells, suggesting that basolateral E2 specifically inhibits apical Ca^{2+} entry in polarized HBECs without affecting ER Ca^{2+} release (Fig. 1*A*).

Little is known regarding the molecular identity of the proteins involved in SOCE in the airway. Therefore, we next determined whether STIM1 and Orai1 were essential for SOCE in HBECs. Nonpolarized HBECs were transfected with STIM1, Orai1, or scrambled siRNA constructs or treated with vehicle (control). Quantitative PCR measurements indicated that both genes were successfully knocked down (Fig. 1*B*). We then performed Ca^{2+} imaging in these cells. Nonpolarized HBECs were placed in a Ca^{2+}-free Ringer's solution and stimulated with thapsigargin to specifically analyze ER Ca^{2+} dynamics. Knockdown of STIM1 or Orai1 had no effect on ER Ca^{2+} release compared with scrambled siRNA (Fig. 1*C*). However, knockdown of either STIM1 or Orai1 completely abolished SOCE, whereas scrambled siRNA was without effect (Fig. 1*C*). This indicated that STIM1 and Orai1 were essential for SOCE in HBECs. Although these observations were made in nonpolarized HBECs, it is reasonable to assume that STIM1 and Orai1 are necessary for SOCE in polarized HBECs.

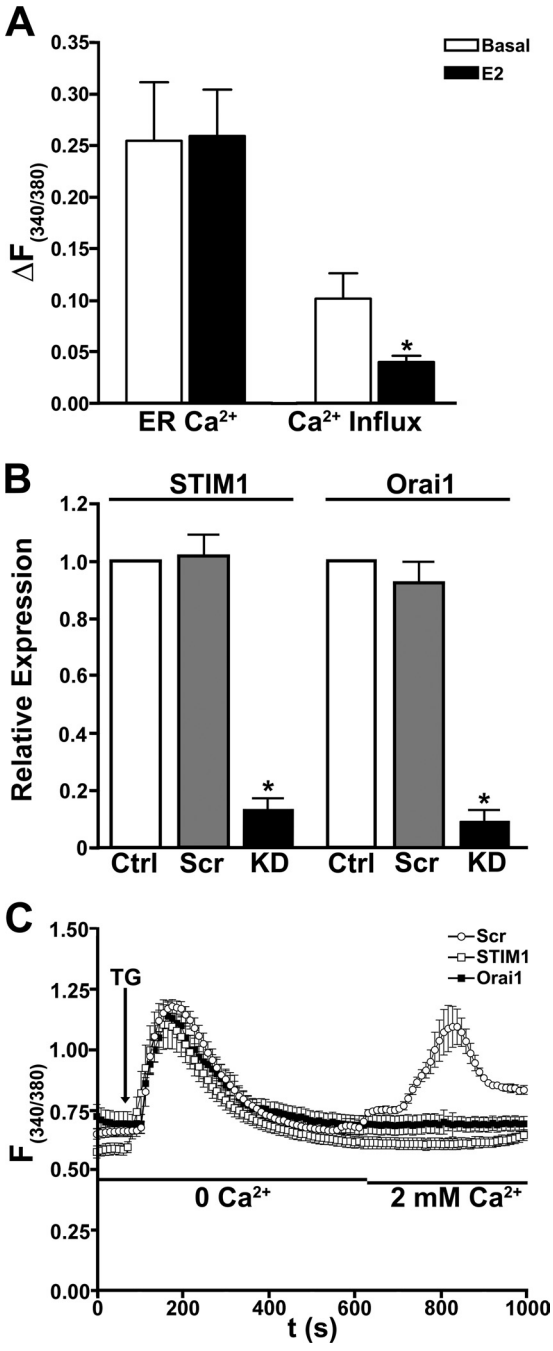

FIGURE 1. **STIM1-dependent Ca^{2+} influx in HBECs is inhibited by E2.** *A*, mean changes in Fura-2 emission ratio in polarized HBECs under control conditions or exposed to 10 nM E2 for 15 min. HBECs were placed in bilateral Ca^{2+}-free Ringer's and stimulated with 2 μM thapsigargin to monitor ER Ca^{2+} depletion. 2 mM Ca^{2+} was added back to the Ringer's solution on the apical surface only to induce SOCE. *B*, relative expression of STIM1 or Orai1 after siRNA knockdown, as indicated by quantitative PCR. Nonpolarized HBECs were treated with transfection reagent alone (*Ctrl*) or transfected with scrambled (*Scr*) or targeted knockdown (*KD*) siRNA constructs. *C*, Fura-2 emission ratio in nonpolarized HBECs that were transfected with scrambled, STIM1, or Orai1 siRNA constructs. SOCE was measured by adding extracellular Ca^{2+} back to the Ringer's solution after ER Ca^{2+} depletion with 2 μM thapsigargin. Data are shown as mean ± S.E.

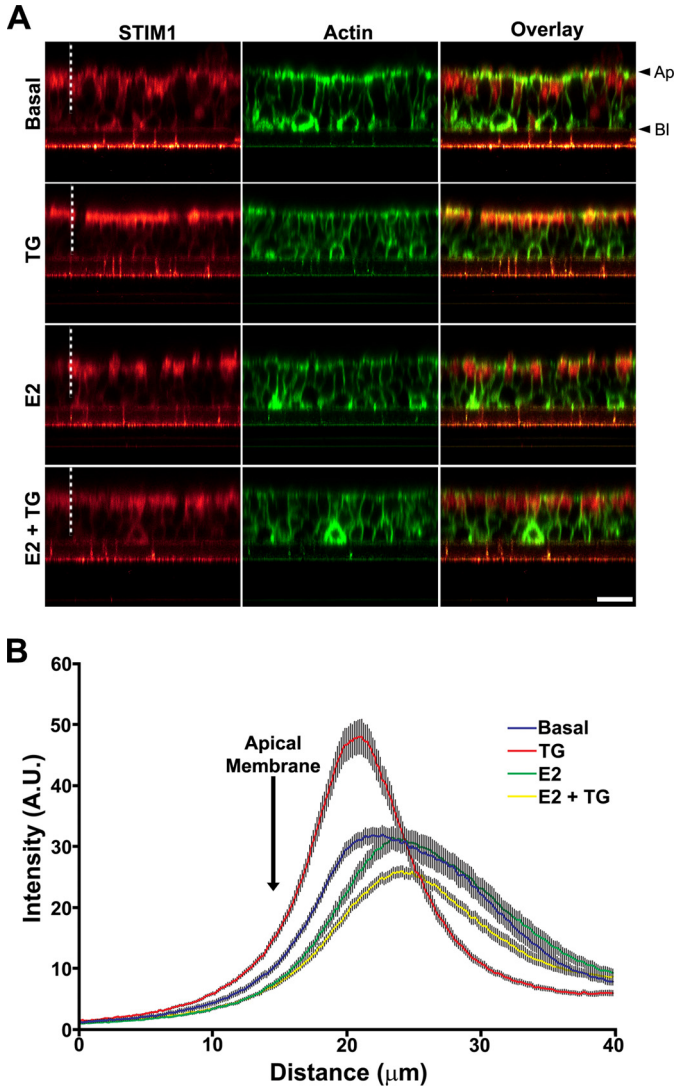

FIGURE 2. **E2 inhibits thapsigargin-induced STIM1 translocation in HBECs.** *A*, typical XZ confocal micrographs of STIM1 immunocytochemistry (*red*) with actin counterstain (phalloidin, *green*). Representative images were from one of several experiments. The cells were either untreated (*Basal*), stimulated with thapsigargin (2 μM) to deplete ER Ca^{2+}, with E2 (10 nM), or with E2 and thapsigargin. *B*, graph of mean pixel intensity of STIM1 in relationship to the apical membrane. Data are shown as mean ± S.E. *Scale bar* represents 25 μm.

E2 Inhibits Translocation of STIM1 to the Apical Membrane in HBECs—We have shown previously that GPCR-mediated IP_3 formation and ER Ca^{2+} release are unaffected by E2 (16). Because STIM1 is next in the SOCE pathway, we tested whether this protein was sensitive to E2. Under basal conditions, STIM1 was found to be diffusely located in polarized HBECs (Fig. 2*A*). However, after thapsigargin-induced ER Ca^{2+} depletion, STIM1 translocated toward the apical membrane. HBECs that were basolaterally pretreated with E2 for 15 min displayed no difference in STIM1 localization compared with untreated cells. However, when ER Ca^{2+} was depleted in cultures pretreated with E2, STIM1 failed to translocate apically (Fig. 2*A*). Data from several experiments were quantified by measuring STIM1 fluorescence intensity using an actin counterstain as a marker of polarity (Fig. 2*B*). Analysis of these data revealed that the subapical concentration of STIM1 was significantly reduced after E2 exposure and suggested that E2 interrupted normal STIM1 function.

E2 Inhibits SOCE and STIM1 Oligomerization in HEK293T Cells—To further study the effects of E2/ESR1 on STIM1 function, we performed additional experiments in HEK293T cells. HEK293T cells were transfected with ESR1-mOrange because they do not endogenously express estrogen receptors (19). As seen in HBECs, E2 did not affect ER Ca^{2+} release, but significantly reduced Ca^{2+} influx (Fig. 3, *A* and *B*), suggesting that ESR1-transfected HEK293T cells were a valid model for studying the effects of E2/ESR1 on STIM1 function.

Oligomerization of STIM1 is an essential step in the initiation of SOCE after ER Ca^{2+} depletion (20, 21). Therefore, we sought to determine whether STIM1 oligomerization after ER Ca^{2+} depletion was inhibited by E2. To characterize the effect of E2 on STIM1 oligomerization, we performed acceptor photobleaching FRET. As a positive control, we linked YFP to mCherry with 5 glycines, which returned a FRET efficiency of ~42% using acceptor photobleaching, which is close to the theoretical maximum of 50% that can be measured with GFP-type proteins ($n = 21$). Conversely, unlinked YFP and mCherry did not undergo FRET ($n = 10$). We then performed FRET between STIM1-YFP and STIM1-mCherry in HEK293T cells. Note: these cells were also expressing ESR1-CFP. However, this construct was only used to verify ESR1 localization and was not excited during acceptor photobleaching. In agreement with previous studies (20, 22–24), we found that STIM1-STIM1 FRET significantly increased after thapsigargin-induced ER Ca^{2+} depletion, suggesting that STIM1 had oligomerized (Fig. 3, *C* and *D*). A 15-min pretreatment with E2 alone did not affect STIM1-STIM1 FRET. However, when cells were pretreated with E2 and then stimulated with thapsigargin, no significant increase in FRET was observed (Fig. 3, *C* and *D*). These data suggest that acute exposure to E2 inhibits STIM1 oligomerization.

E2 Disrupts STIM1 Aggregation and Redistribution—Following oligomerization, STIM1 redistributes to the ER-plasma membrane junction where it interacts with Orai1 and can been seen as puncta (20, 25). To determine whether E2 affects STIM1 puncta formation, we transfected HEK293T cells with STIM1-mCherry and ESR1-CFP and collected images before and after ER Ca^{2+} depletion in the presence/absence of E2 (Fig. 4*A*). We did not observe STIM1 puncta under basal conditions, whereas after ER Ca^{2+} depletion, STIM1 formed puncta in ~90% of the cells (Fig. 4, *A* and *B*). E2 alone did not induce STIM1 puncta formation. However, in the presence of E2, STIM1 puncta formation was significantly decreased after ER Ca^{2+} depletion, suggesting that its ability to oligomerize had been impaired (Fig. 4, *A* and *B*).

We next performed FRET studies between STIM1 and Orai1. Under control conditions, STIM1-Orai1 FRET significantly increased after ER Ca^{2+} depletion as described previously (23). This indicated that STIM1 and Orai1 were in close proximity. However, this increase in FRET was abolished by a 15-min E2 pretreatment, suggesting that E2 prevented STIM1 from interacting with Orai1 (Fig. 4, *C* and *D*). Because STIM1 oligomerization precedes the STIM1-Orai1 interaction, it is likely that loss of STIM1-Orai1 FRET in cells pretreated with E2

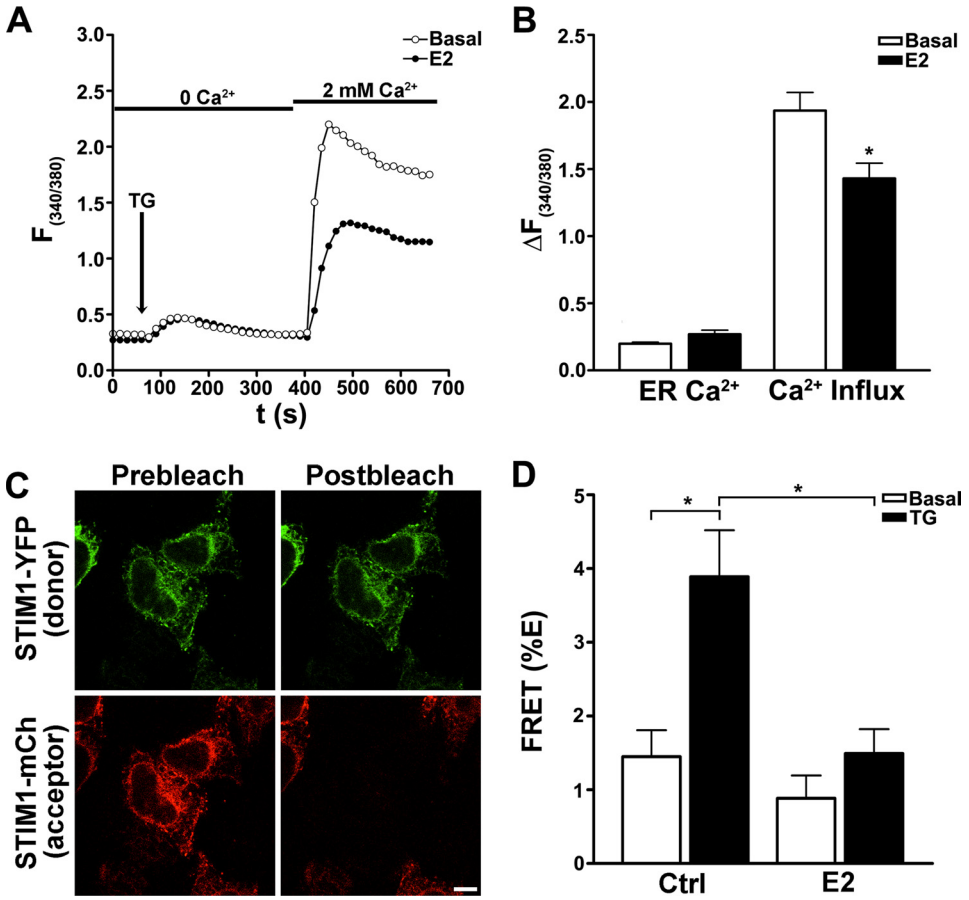

FIGURE 3. **E2 inhibits SOCE and STIM1 oligomerization in HEK293T cells.** *A*, typical changes in Fura-2 emission ratio in HEK293T cells acutely exposed to vehicle or E2 in Ca^{2+}-free Ringer's solution and when 2 mM Ca^{2+} was added back to the Ringer's solution. *B*, mean differences in Fura-2 emission ratio taken from *A*. *, significant difference (unpaired *t* test; $p = 0.0049$). Control (*white bars*), both $n = 53$; E2 (*black bars*), both $n = 57$. *C*, typical confocal micrographs of STIM1-YFP (*green*, donor) and STIM1-mCherry (*red*, acceptor) before and after photobleaching of STIM1-mCherry in control cells under basal conditions. Cells were also expressing ESR1-CFP (data not shown). *D*, mean STIM1-STIM1 FRET efficiency (%*E*) in HEK293T cells. *Ctrl*, basal $n = 31$, *TG* $n = 35$; *E2*, basal $n = 26$, TG $n = 25$. *, significant difference (one-way ANOVA followed by Tukey's multiple comparison test; $p < 0.001$). Data are shown as mean ± S.E. *Scale bar* represents 10 μm.

is a result of inhibiting STIM1 oligomerization. However, we cannot exclude the possibility that E2/ESR1 also independently affect Orai1.

STIM1 Mobility within the ER Is Inhibited by E2—Because E2 impaired the ability of STIM1 to oligomerize and interact with Orai1 (Figs. 3 and 4), we characterized the effects of E2 on STIM1 mobility. Previous studies have utilized FRAP to demonstrate that STIM1 is highly mobile under basal conditions (20). However, upon ER Ca^{2+} depletion, STIM1 mobility significantly decreased (20). FRAP experiments were performed on HEK293T cells co-expressing YFP-STIM1 and ESR1-CFP (Fig. 5*A*). Under basal conditions, we observed an ~80% recovery of STIM1 into the bleached area (Fig. 5, *B* and *C*). However, when ER Ca^{2+} was depleted with thapsigargin, the recovery of STIM1 decreased significantly by ~50% postbleaching, indicating that STIM1 became less mobile (Fig. 5, *B* and *C*), in agreement with previous reports (20, 26). We then repeated this protocol on cells pretreated with E2. Under basal conditions (*i.e.* with full ER stores), E2 significantly reduced STIM1 mobility (Fig. 5, *B* and *C*), suggesting that E2 exposure disrupts STIM1 mobility before STIM1 can sense changes in ER Ca^{2+} levels. Following E2 exposure, thapsigargin only exerted a small additional effect on STIM1 mobility (Fig. 5, *B* and *C*). To ensure that E2 inhibited STIM1 mobility through ESR1, we performed the same experiment on cells only expressing YFP-STIM1 but not ESR1 (Fig. 5, *D* and *E*). Under these conditions, we found that E2 did not affect STIM1 mobility; however, the thapsigargin response was normal. This coincides with our previous observation that E2 decreases cytoplasmic Ca^{2+} specifically through ESR1 in baby hamster kidney cells (16).

EB1 Mobility Is Not Affected by E2—STIM1 translocates along microtubules by associating with the microtubule plus-end tracking protein EB1 (27). Therefore, it is possible that the decrease in STIM1 mobility after E2 exposure was due to a decrease in EB1 mobility. To test this, we performed FRAP studies on HEK293T cells co-expressing EB1-GFP and ESR1-CFP. We found no change in EB1 mobility after ER Ca^{2+} depletion or exposure to E2 (Fig. 6). These data suggest that E2/ESR1 is directly impacting STIM1 without affecting microtubule turnover.

E2 Inhibits Basal Phosphorylation of STIM1—STIM1 contains several serine phosphorylation sites within its C-terminal domain that affect STIM1 function (28, 29). To determine whether E2/ESR1 exerted their influence on STIM1 by modulating the phosphorylation status of the latter, we used an anti-GFP antibody that recognizes YFP to immunoprecipitate YFP-

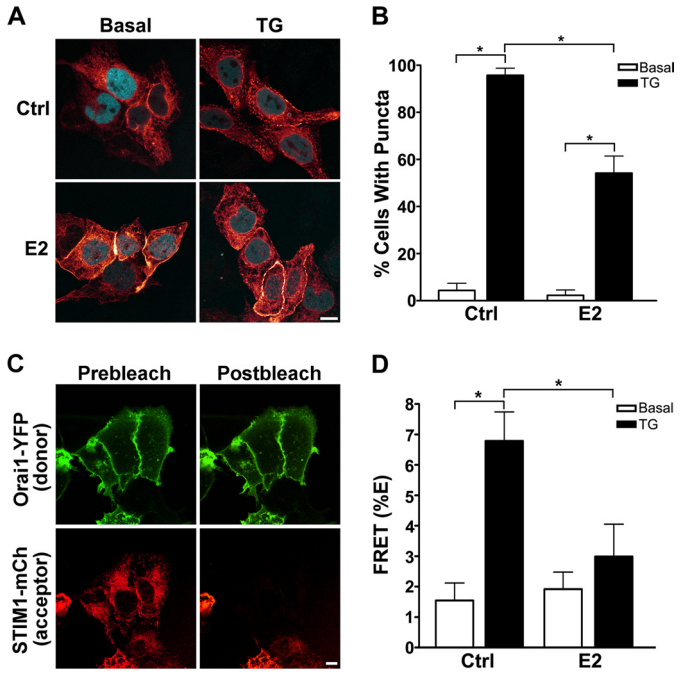

FIGURE 4. **E2 inhibits STIM1 aggregation and redistribution.** *A*, typical images of STIM1-mCherry (*red*) and ESR1-CFP (*cyan*) in HEK293T cells under control or E2 pretreatment conditions ± TG. *B*, percentage of HEK293T cells containing STIM1 puncta. *Ctrl*, basal $n = 46$, TG $n = 47$; *E2*, basal $n = 45$, TG $n = 48$. *C*, typical confocal micrographs of Orai1-YFP (*green*, donor) and STIM1-mCherry (*red*, acceptor) before and after photobleaching of STIM1-mCherry in control cells under resting conditions. Cells also expressed ESR1-CFP (data not shown). *D*, mean STIM1-Orai1 FRET efficiency (%*E*) in HEK293T cells. *Ctrl*, basal $n = 39$, TG $n = 31$; *E2*, basal $n = 39$, TG $n = 33$. *, significant difference (one-way ANOVA followed by Tukey's multiple comparison test; $p < 0.001$). Data are shown as mean ± S.E. *Scale bars* represent 10 μm.

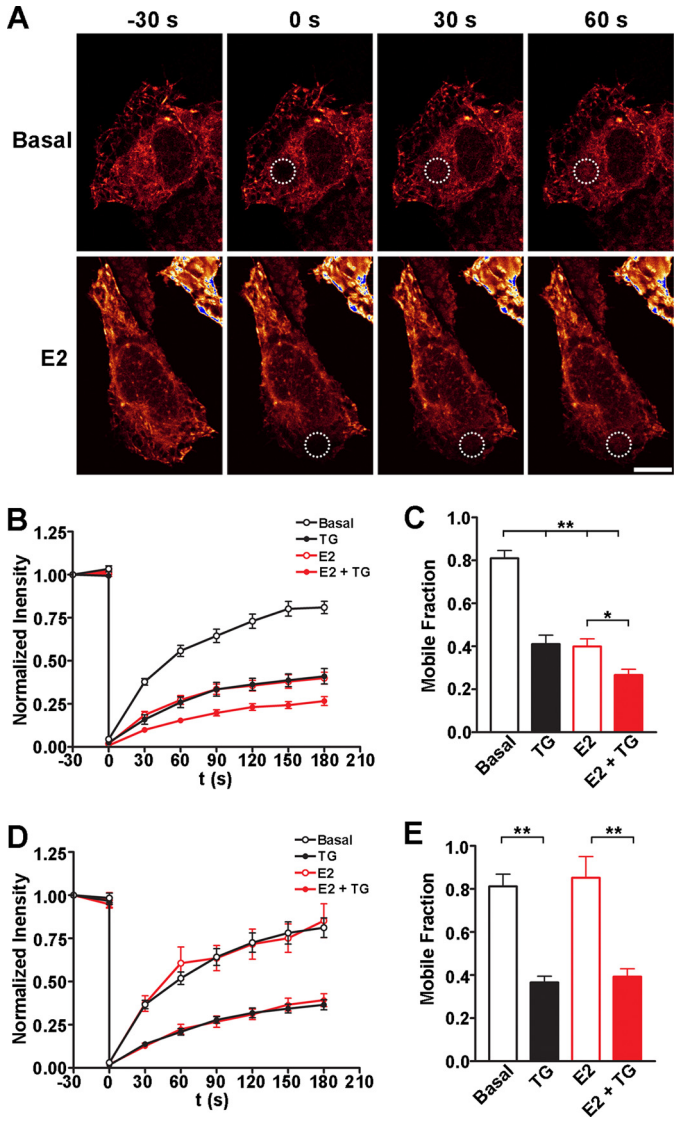

FIGURE 5. **E2 inhibits STIM1 mobility.** *A*, typical images of YFP-STIM1 in HEK293T cells before and after photobleaching (ESR1-CFP not shown). *Dashed circles* indicate the area that was bleached. *B*, normalized recovery of YFP-STIM1 after photobleaching in HEK293T cells co-expressing ESR1-CFP under basal conditions ($n = 15$) and after thapsigargin stimulation ($n = 13$) or when pretreated with E2 ($n = 17$) and after E2 with thapsigargin ($n = 16$). *C*, mobile fraction of YFP-STIM1 in HEK293T cells co-expressing ESR1 under each condition. *D*, normalized recovery of YFP-STIM1 after photobleaching in HEK293T under basal conditions ($n = 13$) and after thapsigargin stimulation ($n = 10$) or when pretreated with E2 ($n = 9$) and after thapsigargin stimulation ($n = 10$). *E*, mobile fraction of YFP-STIM1 in HEK293T cells under each condition. *, significant difference of $p < 0.05$; **, significant difference of $p < 0.001$ (one-way ANOVA followed by Tukey's multiple comparison test). Data are shown as mean ± S.E. *Scale bar* represents 10 μm.

STIM1 from HEK293T cells that co-expressed ESR1. The serine phosphorylation status of STIM1 was then probed using the mpm-2 antibody that specifically recognizes phosphorylated serines that are followed by a proline as described previously (29). All known serine phosphorylation sites in STIM1 are followed by a proline; therefore, the mpm-2 antibody should theoretically detect phosphorylation on every known serine phosphorylation site. In the absence of E2, we observed a distinct band at the predicted mass for YFP-STIM1 (97 kDa, Fig. 7*A*), indicating that STIM1 was phosphorylated. Cells were then exposed to E2 for 5, 10, and 15 min to determine whether the serine phosphorylation status was altered. After a 10-min exposure to E2, we observed a significant decrease in STIM1 phosphorylation, and by 15 min, phosphorylation was almost completely abolished (Fig. 7, *A* and *B*). Although we observed a rapid inhibition of STIM1 phosphorylation, it was also important to determine whether the inhibitory action of E2 was persistent. Therefore, we performed an additional experiment where cells were exposed to E2 for up to 2 h (Fig. 7, *C* and *D*). STIM1 phosphorylation was fully inhibited by 15 min and remained inhibited during the entire time course, suggesting that E2-mediated inhibition of STIM1 phosphorylation is not transient.

To determine where the phosphorylation site(s) were located, we measured phosphorylation in a STIM1 truncation mutant that terminated at amino acid 570 ($STIM1^{570STOP}$) (29). We observed a significant reduction in phosphorylation both basally and following E2 exposure with this mutant, indicating that the serine phosphorylation site was located toward the C terminus of STIM1 (Fig. 7, *E* and *F*). The lack of phosphorylation with $STIM1^{570STOP}$ also acted as a control to confirm that the YFP tag was not being phosphorylated. Because we observed a decrease in phosphorylation after E2 pretreatment, we hypothesized that basal phosphorylation was being inhibited. Serines 575, 608, and 621 are phosphorylated and are required to allow activation of SOCE (28). As a first step toward testing whether these serines were affected by E2/ESR1, we constructed a YFP-STIM1 point mutant where serine 575 was

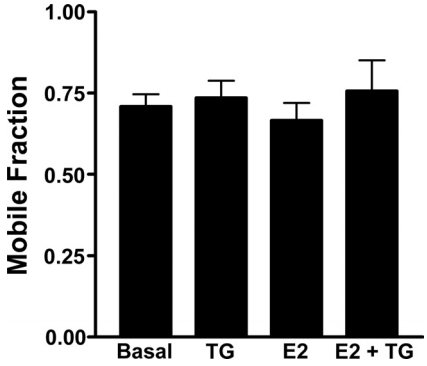

FIGURE 6. **E2 does not alter EB1 mobility.** *Bar graph* shows the mobile fraction of EB1-GFP in HEK293T cells after photobleaching. Cells also expressed ESR1-CFP. All conditions, $n = 8$. Data are shown as mean ± S.E.

mutated to an alanine ($STIM1^{S575A}$). Basal phosphorylation of $STIM1^{S575A}$ was significantly decreased compared with WT STIM1 (Fig. 7, *E* and *F*). Importantly, there was no further decrease in phosphorylation of $STIM1^{S575A}$ when exposed to E2. Additional point mutants at Ser-608 and Ser-621 (*i.e.* $STIM1^{S575A/S608A/S621A}$) did not decrease STIM1 phosphorylation further (data not shown), suggesting that Ser-575 is the phosphorylation site that is affected by E2/ESR1.

We next performed FRAP studies on $STIM1^{S575A}$ to determine whether removal of this phosphorylation site affected STIM1 mobility (Fig. 7, *G* and *H*). $STIM1^{S575A}$ was significantly less mobile than WT STIM1 under basal conditions (Fig. 7*H*). Furthermore, treatment with thapsigargin or E2 had no additional effect on $STIM1^{S575A}$ mobility. These data suggest that loss of STIM1 phosphorylation at Ser-575 by E2/ESR1 induces impaired STIM1 mobility, leading to reduced SOCE. The mobility of the triple point mutant, $STIM1^{S575A/S608A/S621A}$, was not different from $STIM1^{S575A}$ (data not shown). Overall, these data indicate that phosphorylation of Ser-575 is crucial for normal STIM1 function and that a change in the STIM1 phosphorylation status by E2/ESR1 is a mode of regulation for this protein.

DISCUSSION

Many biological processes are initiated by rises in cytoplasmic Ca^{2+}. Thus, regulation of intracellular Ca^{2+} levels is extremely important for normal cellular function (1). We have shown previously that E2 inhibits Ca^{2+} activated Cl^- secretion in airway epithelia by obstructing Ca^{2+} influx (16); however, the pathway utilized by E2 to disrupt this process was not known. Here, we show that acute exposure to E2 inhibits translocation of STIM1 to the apical membrane region in polarized HBECs after ER Ca^{2+} depletion (Fig. 2). Together with calcium imaging experiments in polarized HBECs (Fig. 1), our findings suggest that SOCE occurs at the apical membrane in polarized HBECs and is specifically inhibited by E2. These findings complement previously published data that indicated that SOCE can occur at the apical membrane in nasal epithelial cells (30). Paradiso *et al.* demonstrated that Ca^{2+} influx was itself polarized and was ipsilateral to the stimulus (30).

Previous studies have shown that under resting conditions, STIM1 exists as a dimer that oligomerizes into a higher order complex immediately after ER Ca^{2+} depletion (20, 31). Several studies have utilized FRET to measure oligomerization (20, 25). An increase in FRET efficiency after ER Ca^{2+} depletion is suggestive of STIM1 oligomerization. However, FRET only shows proximity and does not confirm an interaction. In our studies, we found that acute exposure to E2 inhibited the thapsigargin-mediated FRET increase, suggesting that oligomerization was hindered (Fig. 3). It is important to note that E2 alone had no effect on STIM1-STIM1 FRET under resting conditions; however, STIM1 mobility was significantly decreased (Fig. 5), suggesting that the resting oligomeric structure of STIM1 was not affected by E2. Therefore, it is possible that E2 only affects STIM1 aggregation after ER Ca^{2+} depletion and not the resting oligomeric structure. Following oligomerization, STIM1 translocates to the ER-plasma membrane junction where it aggregates into distinct puncta and interacts with Orai1. Our results indicated that E2 inhibited the formation of puncta after ER Ca^{2+} depletion, which coincided with a decrease in STIM1-Orai1 FRET (Fig. 4). Because STIM1 oligomerization precedes puncta formation and the STIM1-Orai1 interaction, it is likely that the observations in Fig. 4 are a result of inhibiting STIM1 oligomerization. STIM1 is also known to interact with members of the transient receptor potential (TRP) superfamily, which can form calcium-permeable channels (32). The exact role of TRP channels in SOCE is not fully understood. However, TRPC1, 3, and 4 have been shown to enter into a complex with Orai1 and may facilitate Ca^{2+} entry (33, 34). Therefore, we speculate that E2-mediated inhibition of STIM1 oligomerization may also inhibit STIM1-TRP channel interactions.

In our FRAP studies, we observed a significant decrease in the mobile fraction of STIM1 after thapsigargin-induced ER Ca^{2+} depletion, which is consistent with previously published data (20). This finding may be due to STIM1 aggregates interacting with the plasma membrane and/or Orai1. To our surprise, E2 alone decreased the mobile fraction of STIM1 without inducing puncta formation. Because STIM1 aggregation precedes translocation to the ER-plasma membrane junction, it is unlikely that E2 decreased STIM1 mobility by inducing a plasma membrane interaction. However, it is possible that E2 altered a STIM1-protein interaction that decreased mobility under resting conditions. Several studies have shown that cytoskeletal proteins, such as tubulin and actin, can interact with or impact STIM1 function (27, 35–37). Previous studies have shown that the microtubule plus-end tracking protein EB1 links STIM1 to the microtubule network and is likely involved in reorganizing the ER (27, 36). Therefore, it is possible that E2/ESR1 was impacting EB1 function and not STIM1. However, our FRAP studies indicated that E2/ESR1 had no effect on EB1 mobility, suggesting a more direct impact on STIM1 (Fig. 6). Nevertheless, it is possible that E2 could affect interactions between STIM1 and the cytoskeleton to inhibit mobility under resting conditions.

Several recent studies have shown that serine phosphorylation can regulate STIM1 and SOCE (28, 29, 36). For example, during mitosis, SOCE is inhibited by phosphorylating STIM1 on Ser-486 and Ser-668 (29). Conversely, phosphorylation of STIM1 on Ser-575, Ser-608, and Ser-621 is required for SOCE (28). This suggests that the site of phosphorylation can greatly influence STIM1 function. In our studies, we found that

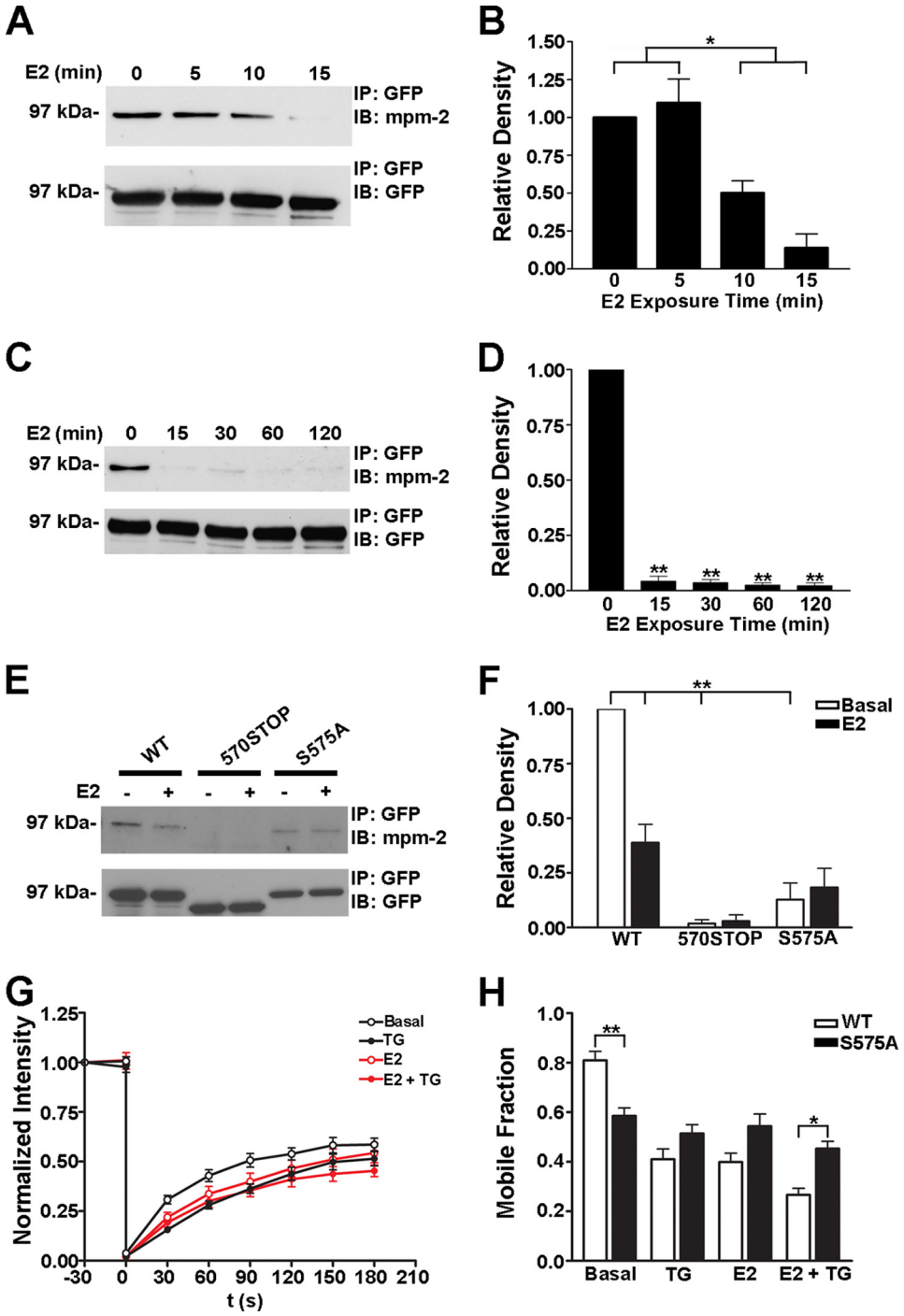

FIGURE 7. **E2 inhibits phosphorylation of STIM1 serine residues.** *A*, E2 rapidly inhibits STIM1 serine phosphorylation. YFP-STIM1 was immunoprecipitated (*IP*) from HEK293T cells co-expressing ESR1 before and after short term E2 exposure. Membranes were probed with the mpm-2 antibody that specifically recognizes phosphorylated serines. The blot was stripped and re-probed with a GFP antibody to reveal total immunoprecipitated STIM1. *IB*, immunoblotting. *B*, relative density of STIM1 phosphorylation for each time point, all $n = 3$. Relative density for phosphorylated STIM1 was calculated by normalizing to total immunoprecipitated STIM1 and comparing it with WT STIM1 under basal conditions. *C*, long lasting inhibition of STIM1 serine phosphorylation. YFP-STIM1 was immunoprecipitated from HEK293T cells co-expressing ESR1 before and after long term E2 exposure. *D*, relative density of STIM1 phosphorylation for each time point, all $n = 4$. *E*, WT YFP-STIM1, STIM1^{570STOP}, and STIM1^{S575A} immunoprecipitated from HEK293T cells co-expressing ESR1. *F*, relative density of STIM1 phosphorylation for each STIM1 construct under basal conditions or after E2 treatment. YFP-STIM1, $n = 11$; STIM1^{570STOP}, $n = 4$; STIM1^{S575A}, $n = 6$. *G*, mean recovery of STIM1^{S575A} into the bleached area following FRAP. Basal, $n = 19$; thapsigargin, $n = 12$; E2, $n = 11$; E2 + thapsigargin, $n = 10$. *H*, mobile fraction of STIM1^{S575A} after photobleaching (*black bars*) compared with WT STIM1 (*white bars*). All FRAP data were collected concurrently. *, significant difference of $p < 0.05$; **, significant difference of $p < 0.001$(one-way ANOVA followed by Tukey's multiple comparison test). Data are shown as mean ± S.E.

E2/ESR1 inhibited basal phosphorylation of STIM1 on Ser-575, which occurred rapidly and was long lasting (Fig. 7, *A–F*). Furthermore, mutation of this residue to an alanine significantly decreased STIM1 mobility (Fig. 7, *G* and *H*), replicating the effects of E2/ESR1. However, we cannot rule out the possibility that other serine phosphorylation sites are being affected by E2/ESR1, but may not be detectable with the mpm-2 antibody. Furthermore, the exact mechanism utilized by E2/ESR1 to

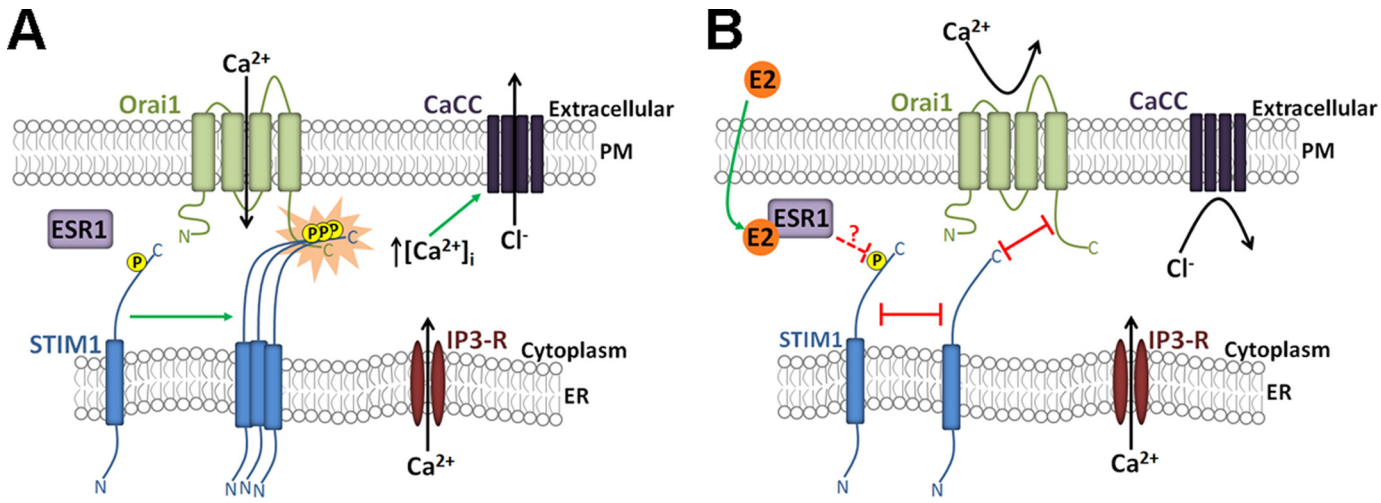

FIGURE 8. **Model depicting the effects of E2 on SOCE in airway epithelia.** *A*, model of SOCE after ER Ca^{2+} depletion in the absence of E2. Phosphorylated STIM1 oligomerizes and interacts with Orai1 to induce SOCE. Elevations in cytoplasmic Ca^{2+} then lead to activation of CaCC. *B*, proposed model of E2/ESR1-mediated inhibition of STIM1 and SOCE after ER Ca^{2+} depletion. E2/ESR1 inhibits STIM1 phosphorylation via an unknown mechanism. This inhibits STIM1 oligomerization, redistribution, and interaction with Orai1 to block SOCE. Low cytoplasmic Ca^{2+} reduces CaCC activation.

inhibit serine phosphorylation remains unknown. Estrogen receptors have typically been described as regulators of gene transcription (38). However, it is well established that estrogen receptors can also signal nongenomically (38, 39). For example, signaling through ESR1 has been shown to impact the PI3K/Akt and ERK1/2 cascades (39, 40). Conversely, E2/ESR1 may activate a phosphatase to dephosphorylate STIM1.

Gender is a risk factor for most lung diseases, including asthma, CF, and COPD. Bronchoconstriction (41), mast cell degranulation (42), and mucus hypersecretion (43) are characteristics of asthma that are Ca^{2+}-regulated, and E2/ESR1 has been shown to act as a bronchodilator in human airway smooth muscle cells by decreasing intracellular Ca^{2+} levels (44). This suggests that E2 is airway-protective in asthma. However, there are many other characteristics of asthma that may be affected by E2/ESR1, including airway smooth muscle hyperplasia and hypertrophy, goblet cell hyperplasia, and inflammation. COPD also disproportionately affects women, and 80% of early onset COPD patients are female (13). Characteristics of COPD include abnormal ion transport, goblet cell hyperplasia, and mucus dehydration (45). Women with CF are also known to suffer more severely than their male counterparts (11, 12, 46, 47), have a higher mortality (11, 47), and are more likely to experience acute exacerbations when E2 is highest during the periovulatory period (12, 46). Sex differences such as those seen in asthma, COPD, and CF are likely to be very complex. However, E2/ESR1-mediated inhibition of STIM1 may play a role in affecting the severity of all of these diseases. In the case of bronchoconstriction, reduced Ca^{2+} levels may be protective. Conversely, in the case of altered ion transport, limiting CaCC activity by decreasing Ca^{2+} may further impair the ability to hydrate the airways and so may exacerbate the disease in females (9).

In conclusion, we have demonstrated that E2/ESR1 can inhibit SOCE by regulating STIM1 function. Under normal conditions, phosphorylated STIM1 can sense ER Ca^{2+} depletion, oligomerize, and activate Orai1 (Fig. 8*A*). However, we propose that acute E2 exposure activates ESR1, which signals nongenomically, to inhibit basal phosphorylation of STIM1 (Fig. 8*B*). Consequently, STIM1 is unable to oligomerize after ER Ca^{2+} depletion and fails to activate Orai1, leading to a decrease in SOCE. A better understanding of this process may lead to the development of novel therapeutic strategies to reverse the sex bias in chronic lung disease.

Acknowledgments—We thank T. Elston and J. Kelley for assistance with data analysis.

REFERENCES

1. Berridge, M. J., Bootman, M. D., and Roderick, H. L. (2003) Calcium signalling: dynamics, homeostasis and remodelling. *Nat. Rev. Mol. Cell Biol.* **4,** 517–529
2. Rizzuto, R., De Stefani, D., Raffaello, A., and Mammucari, C. (2012) Mitochondria as sensors and regulators of calcium signalling. *Nat. Rev. Mol. Cell Biol.* **13,** 566–578
3. Smyth, J. T., Hwang, S. Y., Tomita, T., DeHaven, W. I., Mercer, J. C., and Putney, J. W. (2010) Activation and regulation of store-operated calcium entry. *J. Cell. Mol. Med.* **14,** 2337–2349
4. Roos, J., DiGregorio, P. J., Yeromin, A. V., Ohlsen, K., Lioudyno, M., Zhang, S., Safrina, O., Kozak, J. A., Wagner, S. L., Cahalan, M. D., Veliçelebi, G., and Stauderman, K. A. (2005) STIM1, an essential and conserved component of store-operated Ca^{2+} channel function. *J. Cell Biol.* **169,** 435–445
5. Zhang, S. L., Yu, Y., Roos, J., Kozak, J. A., Deerinck, T. J., Ellisman, M. H., Stauderman, K. A., and Cahalan, M. D. (2005) STIM1 is a Ca^{2+} sensor that activates CRAC channels and migrates from the Ca^{2+} store to the plasma membrane. *Nature* **437,** 902–905
6. Feske, S., Gwack, Y., Prakriya, M., Srikanth, S., Puppel, S. H., Tanasa, B., Hogan, P. G., Lewis, R. S., Daly, M., and Rao, A. (2006) A mutation in Orai1 causes immune deficiency by abrogating CRAC channel function. *Nature* **441,** 179–185
7. Vig, M., Peinelt, C., Beck, A., Koomoa, D. L., Rabah, D., Koblan-Huberson, M., Kraft, S., Turner, H., Fleig, A., Penner, R., and Kinet, J. P. (2006) CRACM1 is a plasma membrane protein essential for store-operated Ca^{2+} entry. *Science* **312,** 1220–1223
8. Soboloff, J., Rothberg, B. S., Madesh, M., and Gill, D. L. (2012) STIM proteins: dynamic calcium signal transducers. *Nat. Rev. Mol. Cell Biol.* **13,** 549–565
9. Tarran, R., Button, B., and Boucher, R. C. (2006) Regulation of normal and cystic fibrosis airway surface liquid volume by phasic shear stress. *Annu.*

Rev. Physiol. **68,** 543–561
10. Townsend, E. A., Miller, V. M., and Prakash, Y. S. (2012) Sex differences and sex steroids in lung health and disease. *Endocr. Rev.* **33,** 1–47
11. Rosenfeld, M., Davis, R., FitzSimmons, S., Pepe, M., and Ramsey, B. (1997) Gender gap in cystic fibrosis mortality. *Am. J. Epidemiol.* **145,** 794–803
12. Chotirmall, S. H., Smith, S. G., Gunaratnam, C., Cosgrove, S., Dimitrov, B. D., O'Neill, S. J., Harvey, B. J., Greene, C. M., and McElvaney, N. G. (2012) Effect of estrogen on pseudomonas mucoidy and exacerbations in cystic fibrosis. *N. Engl. J. Med.* **366,** 1978–1986
13. Silverman, E. K., Weiss, S. T., Drazen, J. M., Chapman, H. A., Carey, V., Campbell, E. J., Denish, P., Silverman, R. A., Celedon, J. C., Reilly, J. J., Ginns, L. C., and Speizer, F. E. (2000) Gender-related differences in severe, early onset chronic obstructive pulmonary disease. *Am. J. Respir. Crit. Care Med.* **162,** 2152–2158
14. Schatz, M., and Camargo, C. A., Jr. (2003) The relationship of sex to asthma prevalence, health care utilization, and medications in a large managed care organization. *Ann. Allergy Asthma Immunol.* **91,** 553–558
15. Siegfried, J. M. (2001) Women and lung cancer: does oestrogen play a role? *Lancet Oncol.* **2,** 506–513
16. Coakley, R. D., Sun, H., Clunes, L. A., Rasmussen, J. E., Stackhouse, J. R., Okada, S. F., Fricks, I., Young, S. L., and Tarran, R. (2008) 17β-Estradiol inhibits Ca^{2+}-dependent homeostasis of airway surface liquid volume in human cystic fibrosis airway epithelia. *J. Clin. Invest.* **118,** 4025–4035
17. Randell, S. H., Fulcher, M. L., O'Neal, W., and Olsen, J. C. (2011) Primary epithelial cell models for cystic fibrosis research. *Methods Mol. Biol.* **742,** 285–310
18. Sheridan, J. T., Worthington, E. N., Yu, K., Gabriel, S. E., Hartzell, H. C., and Tarran, R. (2011) Characterization of the oligomeric structure of the Ca^{2+}-activated Cl^- channel Ano1/TMEM16A. *J. Biol. Chem.* **286,** 1381–1388
19. Thomas, P., Pang, Y., Filardo, E. J., and Dong, J. (2005) Identity of an estrogen membrane receptor coupled to a G protein in human breast cancer cells. *Endocrinology* **146,** 624–632
20. Liou, J., Fivaz, M., Inoue, T., and Meyer, T. (2007) Live-cell imaging reveals sequential oligomerization and local plasma membrane targeting of stromal interaction molecule 1 after Ca^{2+} store depletion. *Proc. Natl. Acad. Sci. U.S.A.* **104,** 9301–9306
21. Luik, R. M., Wang, B., Prakriya, M., Wu, M. M., and Lewis, R. S. (2008) Oligomerization of STIM1 couples ER calcium depletion to CRAC channel activation. *Nature* **454,** 538–542
22. Barr, V. A., Bernot, K. M., Srikanth, S., Gwack, Y., Balagopalan, L., Regan, C. K., Helman, D. J., Sommers, C. L., Oh-Hora, M., Rao, A., and Samelson, L. E. (2008) Dynamic movement of the calcium sensor STIM1 and the calcium channel Orai1 in activated T-cells: puncta and distal caps. *Mol. Biol. Cell* **19,** 2802–2817
23. Navarro-Borelly, L., Somasundaram, A., Yamashita, M., Ren, D., Miller, R. J., and Prakriya, M. (2008) STIM1-Orai1 interactions and Orai1 conformational changes revealed by live-cell FRET microscopy. *J. Physiol.* **586,** 5383–5401
24. Wang, Y., Deng, X., Zhou, Y., Hendron, E., Mancarella, S., Ritchie, M. F., Tang, X. D., Baba, Y., Kurosaki, T., Mori, Y., Soboloff, J., and Gill, D. L. (2009) STIM protein coupling in the activation of Orai channels. *Proc. Natl. Acad. Sci. U.S.A.* **106,** 7391–7396
25. Covington, E. D., Wu, M. M., and Lewis, R. S. (2010) Essential role for the CRAC activation domain in store-dependent oligomerization of STIM1. *Mol. Biol. Cell* **21,** 1897–1907
26. Kilch, T., Alansary, D., Peglow, M., Dörr, K., Rychkov, G., Rieger, H., Peinelt, C., and Niemeyer, B. A. (2013) Mutations of the Ca^{2+}-sensing stromal interaction molecule STIM1 regulate Ca^{2+} influx by altered oligomerization of STIM1 and by destabilization of the Ca^{2+} channel Orai1. *J. Biol. Chem.* **288,** 1653–1664
27. Grigoriev, I., Gouveia, S. M., van der Vaart, B., Demmers, J., Smyth, J. T., Honnappa, S., Splinter, D., Steinmetz, M. O., Putney, J. W., Jr., Hoogenraad, C. C., and Akhmanova, A. (2008) STIM1 is a MT-plus-end-tracking protein involved in remodeling of the ER. *Curr. Biol.* **18,** 177–182
28. Pozo-Guisado, E., Campbell, D. G., Deak, M., Alvarez-Barrientos, A., Morrice, N. A., Alvarez, I. S., Alessi, D. R., and Martín-Romero, F. J. (2010) Phosphorylation of STIM1 at ERK1/2 target sites modulates store-operated calcium entry. *J. Cell Sci.* **123,** 3084–3093
29. Smyth, J. T., Petranka, J. G., Boyles, R. R., DeHaven, W. I., Fukushima, M., Johnson, K. L., Williams, J. G., and Putney, J. W., Jr. (2009) Phosphorylation of STIM1 underlies suppression of store-operated calcium entry during mitosis. *Nat. Cell Biol.* **11,** 1465–1472
30. Paradiso, A. M., Mason, S. J., Lazarowski, E. R., and Boucher, R. C. (1995) Membrane-restricted regulation of Ca^{2+} release and influx in polarized epithelia. *Nature* **377,** 643–646
31. Yang, X., Jin, H., Cai, X., Li, S., and Shen, Y. (2012) Structural and mechanistic insights into the activation of stromal interaction molecule 1 (STIM1). *Proc. Natl. Acad. Sci. U.S.A.* **109,** 5657–5662
32. Salido, G. M., Jardín, I., and Rosado, J. A. (2011) The TRPC ion channels: association with Orai1 and STIM1 proteins and participation in capacitative and noncapacitative calcium entry. *Adv. Exp. Med. Biol.* **704,** 413–433
33. Cioffi, D. L., Wu, S., Chen, H., Alexeyev, M., St Croix, C. M., Pitt, B. R., Uhlig, S., and Stevens, T. (2012) Orai1 determines calcium selectivity of an endogenous TRPC heterotetramer channel. *Circ. Res.* **110,** 1435–1444
34. Woodard, G. E., López, J. J., Jardín, I., Salido, G. M., and Rosado, J. A. (2010) TRPC3 regulates agonist-stimulated Ca^{2+} mobilization by mediating the interaction between type I inositol 1,4,5-trisphosphate receptor, RACK1, and Orai1. *J. Biol. Chem.* **285,** 8045–8053
35. Rosado, J. A., López, J. J., Harper, A. G., Harper, M. T., Redondo, P. C., Pariente, J. A., Sage, S. O., and Salido, G. M. (2004) Two pathways for store-mediated calcium entry differentially dependent on the actin cytoskeleton in human platelets. *J. Biol. Chem.* **279,** 29231–29235
36. Smyth, J. T., Beg, A. M., Wu, S., Putney, J. W., Jr., and Rusan, N. M. (2012) Phosphoregulation of STIM1 leads to exclusion of the endoplasmic reticulum from the mitotic spindle. *Curr. Biol.* **22,** 1487–1493
37. Smyth, J. T., DeHaven, W. I., Bird, G. S., and Putney, J. W., Jr. (2007) Role of the microtubule cytoskeleton in the function of the store-operated Ca^{2+} channel activator STIM1. *J. Cell Sci.* **120,** 3762–3771
38. Osborne, C. K., and Schiff, R. (2005) Estrogen-receptor biology: continuing progress and therapeutic implications. *J. Clin. Oncol.* **23,** 1616–1622
39. Wu, Q., Chambliss, K., Umetani, M., Mineo, C., and Shaul, P. W. (2011) Non-nuclear estrogen receptor signaling in the endothelium. *J. Biol. Chem.* **286,** 14737–14743
40. Wang, M., Crisostomo, P., Wairiuko, G. M., and Meldrum, D. R. (2006) Estrogen receptor-α mediates acute myocardial protection in females. *Am. J. Physiol. Heart Circ. Physiol.* **290,** H2204–2209
41. Huang, F., Zhang, H., Wu, M., Yang, H., Kudo, M., Peters, C. J., Woodruff, P. G., Solberg, O. D., Donne, M. L., Huang, X., Sheppard, D., Fahy, J. V., Wolters, P. J., Hogan, B. L., Finkbeiner, W. E., Li, M., Jan, Y. N., Jan, L. Y., and Rock, J. R. (2012) Calcium-activated chloride channel TMEM16A modulates mucin secretion and airway smooth muscle contraction. *Proc. Natl. Acad. Sci. U.S.A.* **109,** 16354–16359
42. Di Capite, J. L., Bates, G. J., and Parekh, A. B. (2011) Mast cell CRAC channel as a novel therapeutic target in allergy. *Curr. Opin. Allergy Clin. Immunol.* **11,** 33–38
43. Lai, H. Y., and Rogers, D. F. (2010) Mucus hypersecretion in asthma: intracellular signalling pathways as targets for pharmacotherapy. *Curr. Opin Allergy. Clin. Immunol.* **10,** 67–76
44. Townsend, E. A., Sathish, V., Thompson, M. A., Pabelick, C. M., and Prakash, Y. S. (2012) Estrogen effects on human airway smooth muscle involve cAMP and protein kinase A. *Am. J. Physiol. Lung Cell Mol. Physiol.* **303,** L923–928
45. Randell, S. H., and Boucher, R. C. (2006) Effective mucus clearance is essential for respiratory health. *Am. J. Respir. Cell Mol. Biol.* **35,** 20–28
46. Block, J. K., Vandemheen, K. L., Tullis, E., Fergusson, D., Doucette, S., Haase, D., Berthiaume, Y., Brown, N., Wilcox, P., Bye, P., Bell, S., Noseworthy, M., Pedder, L., Freitag, A., Paterson, N., and Aaron, S. D. (2006) Predictors of pulmonary exacerbations in patients with cystic fibrosis infected with multi-resistant bacteria. *Thorax* **61,** 969–974
47. Demko, C. A., Byard, P. J., and Davis, P. B. (1995) Gender differences in cystic fibrosis: *Pseudomonas aeruginosa* infection. *J. Clin. Epidemiol.* **48,** 1041–1049